Chemical Science

Modulating Structure and Properties in Organic Chromophores: Influence of Azulene as a Building Block

Journal:	*Chemical Science*
Manuscript ID:	SC-EDG-06-2014-001623.R1
Article Type:	Edge Article
Date Submitted by the Author:	26-Jun-2014
Complete List of Authors:	Hawker, Craig; University of California, Materials Research Laboratory Murai, Masahito; Okayama University, Division of Chemistry and Biochemistry Ku, Sung-Yu; UCSB, Material Research Laboratory Treat, Neil; University of California, Materials Department Robb, Maxwell; University of California, Department of Chemistry and Biochemistry Chabinyc, Michael L. ; University of California, Santa Barbara, Materials Department

Journal Name

RSCPublishing

ARTICLE

Modulating Structure and Properties in Organic Chromophores: Influence of Azulene as a Building Block

Cite this: DOI: 10.1039/xoxxoooooox

Received ooth January 2012,
Accepted ooth January 2012

DOI: 10.1039/xoxxoooooox

www.rsc.org/

Masahito Murai,[a,d] Sung-Yu Ku,[a] Neil D. Treat,[a,b] Maxwell J. Robb,[a,c] Michael L. Chabinyc,[a,b] and Craig J. Hawker*[a,b,c]

The properties of isomeric azulene derivatives, substituted through the 5-membered ring, were examined using a combination of experimentation and theoretical calculations for a series of well-defined electroactive oligomers. The substitution pattern was shown to dramatically influence solid-state, electronic, and optical properties of the oligomers with acid-responsive materials only being observed when the azulenium cation could be directly stabilized by substituents on the 5-membered ring. In addition, the absorption maxima and optical band-gaps of the azulenium cations can be tuned by the substitution position of the azulene ring by the chromophore.

Introduction

New design strategies for functional organic chromophores are of great interest for the continued development of optoelectronic devices such as organic field-effect transistors (OFETs), organic light-emitting diodes (OLEDs), and dye-sensitized organic solar cells (DSSCs).[1] Significant attention in this area has focused on exploiting a diverse range of modular building blocks to fine-tune electronic and solid state structures with the ultimate goal of optimizing performance and nanoscale morphologies. The most efficient and general strategy developed to date includes the incorporation of heteroatoms, introduction of electron-donating and/or electron-withdrawing substituents into the parent π-conjugated framework, and/or extension of their π-systems by annulation with aromatic compounds leading to PAHs (polycyclic aromatic hydrocarbons).[2] These methods have proved successful; however, chemical instability, especially against oxidation and poor solubility derived from expanded planar π-conjugated systems often limits their scope for further applications.[3] To compensate for these drawbacks, we now introduce a new approach using a pure hydrocarbon building block, azulene, to create novel π-conjugated frameworks with control over the optical properties as well as nanoscale morphology in the solid state.

The choice of azulene as a key building block was driven by its unique aromatic structure consisting of fused seven- and five-membered rings with partial positive and negative charges, respectively. Unlike its constitutional isomer naphthalene, azulene exhibits a bright blue color due to its decreased aromatic resonance energy combined with its strong dipole moment.[4] Furthermore, its low ionization energy and high electron affinity allows for the tuning of physical and electronic properties in a similar fashion to fullerenes.[5] Interesting structural variations include azulene-fused porphyrins and azulenocyanines, which exhibit red-shifted visible absorption derived from their significantly extended π-conjugation.[6] Although these examples highlight the attractive properties of azulene and its ability to create novel π-conjugated systems, the effect of the polarized character of azulene to enhance and control materials properties has not been fully investigated and may offer advantages compared to traditional repeat units.[7]

Recently, we described the synthesis and characterization of various isomeric azulene derivatives substituted in either the 5- or 7-membered ring and observed significantly different properties when substituted in the seven-membered ring leading to stabilization of the corresponding azulenium cations and reversible color changes/fluorescent switching.[8] This ability to obtain stimuli-responsiveness properties in π-conjugated systems based on azulenes is reminiscent of the behavior of polyanilines; however, in the case of polyaniline, protonation occurs at the nitrogen atoms, whereas protonation of azulene systems occurs in the conjugated aromatic backbone resulting in a more pronounced effect on the resulting π-conjugated systems.

Based on these preliminary studies, we envisioned that the optoelectronic and solid state morphological properties of azulene-based π-conjugated systems can be further controlled by: **1)** *enhancement of the polarized structure* through conjugation with a strong electron-acceptor to the electron-rich

five-membered ring of azulene. It should be noted that this approach is not available to more traditional hydrocarbon building blocks such as phenyl or naphthalene derivatives; **2)** *post-synthetic modification by external stimuli* utilizing acid-base and redox reactions.[9] From a device application standpoint, the tunable polarized structure of azulene can also be expected to have several advantages with respect to controlling molecular ordering which is critical for efficient charge transport. Herein, we demonstrate that these approaches make it possible to fine tune the electronic structure, physical properties, and nanoscale morphology of π-conjugated materials by utilizing the enhanced dipole nature of azulene. Azulene-diketopyrrolopyrrole conjugates (AzDPPs) connected through furyl linkers were chosen as target molecules as DPPs are widely studied dyes that have been used as acceptor components in materials for bulk heterojunction solar cells and DSSCs[10] while the furan units impart high solubility and leads to high fluorescence quantum yields.[11]

Results and Discussion

The optical and electronic properties of azulene can be tuned in a facile manner by the introduction of various substituents with the majority of previous reports focusing on functionalization at the 1- or 3-positions. In contrast, functionalization at the 2-position of azulene has been limited[12] due to the tendency of the five-membered ring of azulene to undergo electrophilic substitution exclusively at the 1- or 3-positions because of its unique polarized π-electron system.[13] Traditionally, the introduction of substituents at the 2-position requires multistep syntheses involving construction of the azulene skeleton.[14] Alternatively, functionalization based on nucleophilic halogenation is challenging due to the inherent instability of halogenated azulenes.[15] With this in mind, we focused on the iridium-catalyzed, direct C-H borylation of azulene.[16,17] Significantly, this provides the synthetically useful 2-boryl (as well as the 1-boryl as a side product) derivative from commercially available azulene in a single step (72% yield for 2- and 7% yield for 1-borylazulene, respectively) (Figure 1). From the purified 1- and 2-borylazulene derivatives, two regioisomers 1-AzDPP, **1**, and 2-AzDPP, **2**, were successfully obtained by microwave-assisted Suzuki-Miyaura coupling with the dibromo-substituted 3,6-bis(5-bromofuran-2-yl)pyrrolo[3,4-*c*]pyrrole-1,4-dione (DPP), **3**, in good yields (Figure 1 and Scheme S1 in ESI). To gain fundamental insight into the electronic interaction between azulene and substituent groups, model compounds such as the isomeric naphthalene-DPP conjugate NpDPP, **5**, and corresponding phenylazulene derivatives 2-AzPh, **6**, and 1-AzPh, **7**, were also synthesized (Scheme S2 in ESI). All of the new compounds were fully characterized by ^{1}H NMR, ^{13}C NMR, IR, and HRMS and found

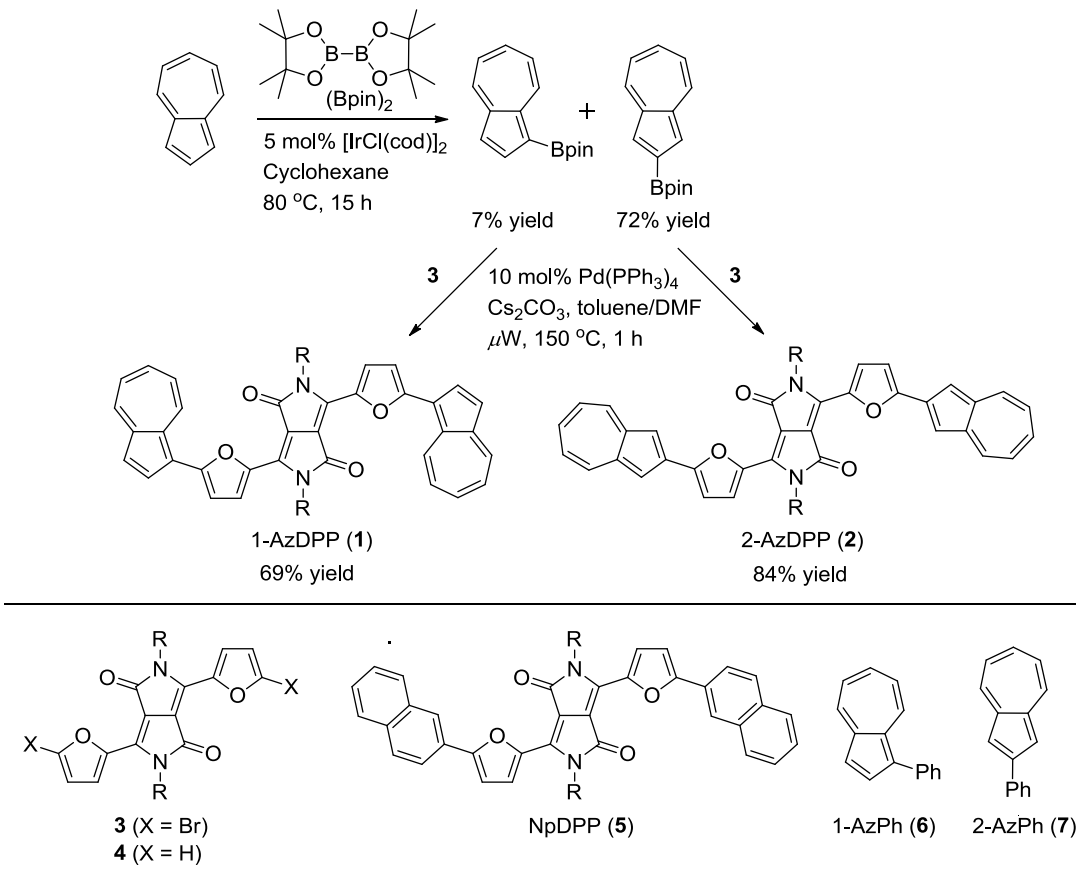

Figure 1. Synthesis of DPP-Azulene conjugates **1** and **2** (R = 2-ethylhexyl), and the structures of model compounds.

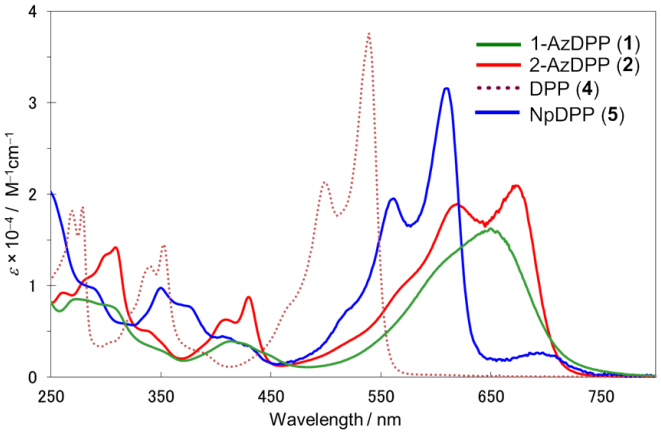

Figure 2. UV-Vis absorption spectra of **1**, **2**, **4** and **5** in CH_2Cl_2 (1×10^{-6} M) at rt.

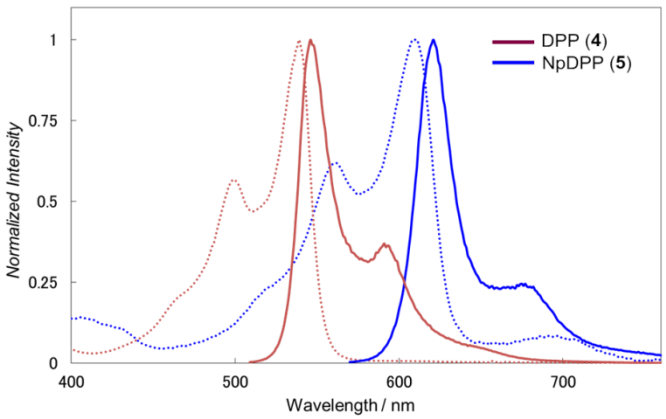

Figure 4. Absorption (dashed line) and fluorescence spectra (solid line) for DPP **4** and NpDPP **5** in CH_2Cl_2 at rt.

to be fully soluble (at least greater than 10 mg/mL) in common organic solvents such as CH_2Cl_2, $CHCl_3$, THF, and toluene at room temperature.

The UV-visible absorption spectra of 1-AzDPP, **1**, 2-AzDPP, **2**, and NpDPP, **5**, in CH_2Cl_2 were compared with the parent DPP derivative, **4**, to evaluate the efficiency of conjugation through the backbone (Figure 2 and Table S1 in ESI). In all cases, 1-AzDPP, 2-AzDPP, and NpDPP exhibit red-shifted absorption in the visible region with respect to **4**, indicating a reduced HOMO-LUMO gap due to the increased π-electron delocalization. It is noteworthy that azulene derivatives, **1** and **2**, display a significant absorption between 550 and 700 nm which is particularly desirable for solar cell and NIR dyes applications.[1] Interestingly, the absorption maximum for 1-AzDPP was blue shifted approximately 40 nm and displayed a single, broad peak when compared with the 2-AzDPP regioisomer.[18] This observation suggests an effective decrease of the energy gap resulting from substitution through the 2-position rather than the 1-position of the azulene ring with the low energy transition of 2-AzDPP exhibiting discreet vibronic structure. Similar modulation in the absorption properties was also observed for model compounds 2-AzPh, **6**, and 1-AzPh, **7** (Figure 3). The lowest energy absorption maximum peak for 2-AzPh (390 nm) is characteristic of the π-π* transition of the azulene rings, which is red-shifted by 20 nm compared with that of the regioisomer 1-AzPh (370 nm), again indicating more effective conjugation through the 2-position of azulene ring.

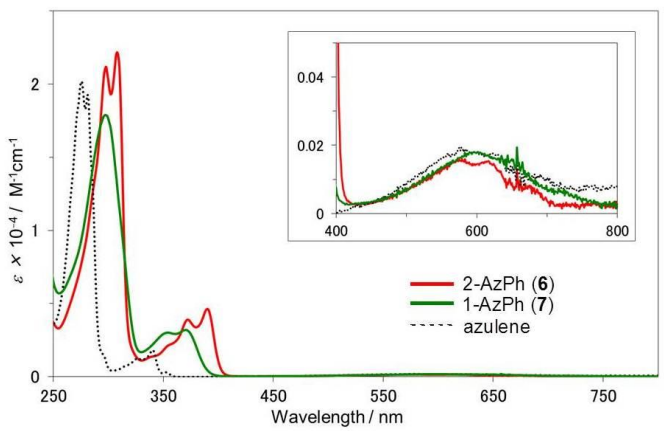

Figure 3. UV-Vis absorption spectra of **6**, **7** and the parent azulene in CH_2Cl_2 (1×10^{-6} M) at rt.

The introduction of azulenyl and naphthyl groups into DPP also induces unique fluorescence behavior. The fluorescence spectrum of NpDPP exhibits a maximum fluorescence band at 621 nm with a shoulder at approximately 677 nm upon excitation at 562 nm (Figure 4).[19] In contrast, no fluorescence emission was observed for 1-AzDPP and 2-AzDPP when excited at ~600 nm.[20] The origin of the lack of emission is unclear at this point. A possible explanation is the formation of a non-emissive intramolecular charge-transfer state of other electronic state formed by a twist of the DPP unit relative to the azulene unit.[19] If the dominant contribution to the electronic state was made by the azulene unit, one might expect a very weak emission based on the poor quantum yield typical of azulene derivatives.[22,23]

To elucidate the influence of the substitution pattern of the azulene ring on the electronic structure and photophysical properties of the above DPP derivatives, truncated structures, **1'**, **2'**, and **5'** were optimized by density function theory (DFT) calculation at the B3LYP/6-31G* level of theory as model compounds for 1-AzDPP, **1**, 2-AzDPP, **2**, and NpDPP, **5**. In each case, the 2-ethylhexyl groups on the nitrogen were replaced by a methyl group to simplify the calculations. As displayed in Figure 4, the LUMO is delocalized over the entire 2-AzDPP framework for **2'**, whereas the corresponding LUMO for NpDPP is mainly localized on the central DPP moiety and the furyl bridge for **5'**. The calculated first excited state for 2-AzDPP, mainly consisting of a HOMO to LUMO transition, has an excitation energy of 1.83 eV (Table S3 in ESI) and replacement of azulene with a naphthalene substituent leads to an increase in the LUMO energy level by 0.22 eV (-2.70 eV for 2-AzDPP *vs* -2.48 eV for NpDPP), whereas the HOMO level remains nearly unchanged (Figure 5). As a result, the calculated first excited energy of NpDPP is increased to 2.09 eV and leads

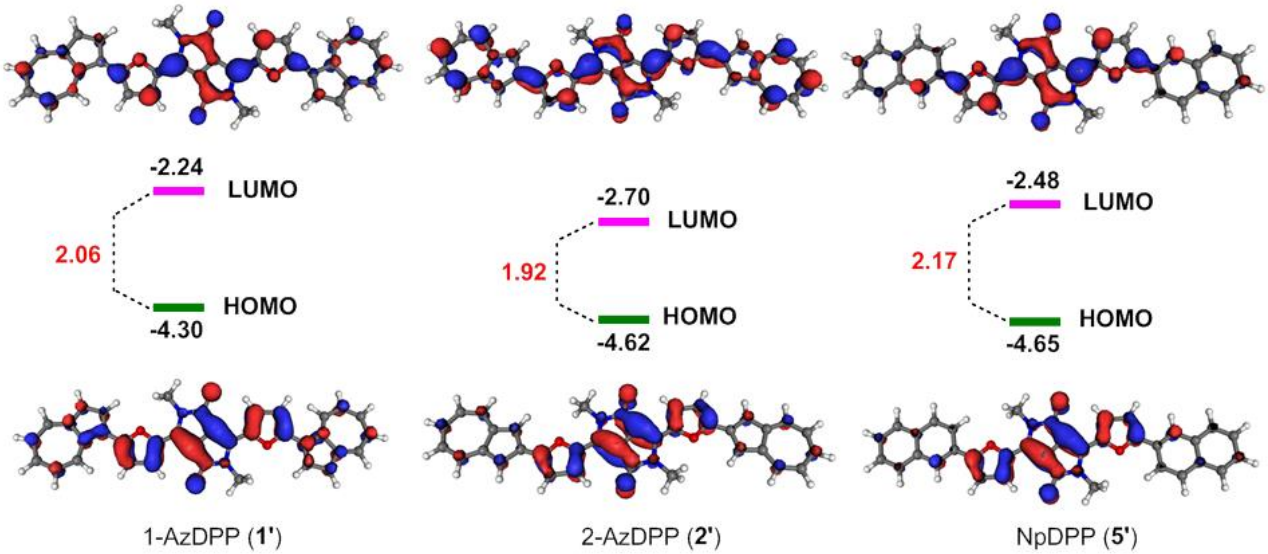

Figure 5. Optimized structure and contour plots of HOMO and LUMO of **1'**, **2'** and **5'**.

to a blue-shifted absorption (Table S4 in ESI). The red-shift of the absorption in 2-AzDPP compared to that of 1-AzDPP can be explained through *stabilization of the LUMO* of the azulene skeleton by the electron-withdrawing ability of the DPP unit with a large distribution at the 2-position of the azulene building block in the LUMO.[24] This result is in sharp contrast to traditional observations for π-systems extended by annulation with aromatics leading to PAHs (polycyclic aromatic hydrocarbons), in which destabilization of the HOMO is the primary reason for decreased bandgaps.[2] The lowest energy conformation of 1-AzDPP, in which the DPP-furan unit is connected at the 1-position of the azulene ring, has a dihedral angle of about 22.4^o between the furan and the azulene units, whereas its isomer 2-AzDPP is essentially planar with a corresponding dihedral angle of less than 2^o. These different geometries also influence the electron delocalization and partially disturb conjugation in 1-AzDPP. The HOMO-LUMO energy gap of 2-AzDPP is smaller than that of 1-AzDPP and NpDPP, which is in good agreement with UV-vis experiments shown in Figure 2.

Azulenes are known to have unique photophysical properties that are sensitive to acid/base chemistry, which stimulated an examination of the UV-visible absorption behavior of 1-AzDPP and 2-AzDPP upon exposure to trifluoroacetic acid (TFA).[4-6] Interestingly, for both isomers dramatically different changes in the absorption spectra were observed in CH_2Cl_2 at room temperature with a minor change in the absorption maximum for 1-AzDPP (ca. 25 nm) compared to a very large shift for 2-AzDPP (ca. 200 nm) (Figure 6).[25] As a control, the parent DPP-furan, **4**, and NpDPP were subjected to the same acid treatment and neither exhibited any change in absorption even in the case of adding a large excess of TFA. This observation indicates that protonation occurs exclusively on the azulene moiety affording the 6π-electron tropylium cation, and not on the nitrogen or oxygen atoms of the DPP unit. Additionally, no EPR signal was observed for both 1-AzDPP and 2-AzDPP in TFA at room temperature. The spectral changes in the visible region can therefore be attributed to the formation of the corresponding azulenium cations and not cation radicals. These results are in sharp contrast to previous reports of azulenes having substituents on the five-membered ring, where the protonation has been reported to generate azulenium cation radicals.[26] This unique behavior can be understood for **1** and **2** due to conjugation with the strongly electron-accepting DPP unit which decreases electron density of the five-membered rings preventing the oxidation of cations to form corresponding cation radicals.[27]

Examining the protonation behavior of 1-AzDPP, **1**, and 2-AzDPP, **2**, in more detail revealed a two-step change in the UV-visible absorption spectra during the course of titration experiments with TFA. For 2-AzDPP, **2**, addition of TFA initially results in a new absorption peak at 833 nm which is gradually blue-shifted to 797 nm and increases in intensity with a well-defined isosbestic point at 695 nm when excess TFA is added (Figure 6, left). In direct contrast, attenuation of the absorption at 646 nm for the regioisomer 1-AzDPP, **1**, was observed with a simultaneous appearance of new peaks at 587 and 629 nm on the addition of TFA (Figure 6, right). These changes in the UV-visible absorption spectra are reflected in a color change of the solutions from blue to green (for 2-AzDPP) and light blue to dark blue (for 1-AzDPP). Step-wise protonation of the two azulene units in **1** and **2** could also be monitored by ^{1}H NMR spectroscopy with downfield shifts of the aromatic protons being observed upon the addition of TFA to 1-AzDPP and 2-AzDPP (4×10^{-3} M in $CDCl_3$) (Figure S1 and S2 in ESI). Notably, neutralization of the TFA solutions of 1-AzDPP and 2-AzDPP with triethylamine resulted in the reproduction of the initial UV-visible spectra in the neutral states, indicating that protonation is completely reversible which was also confirmed by ^{1}H NMR spectroscopy (See

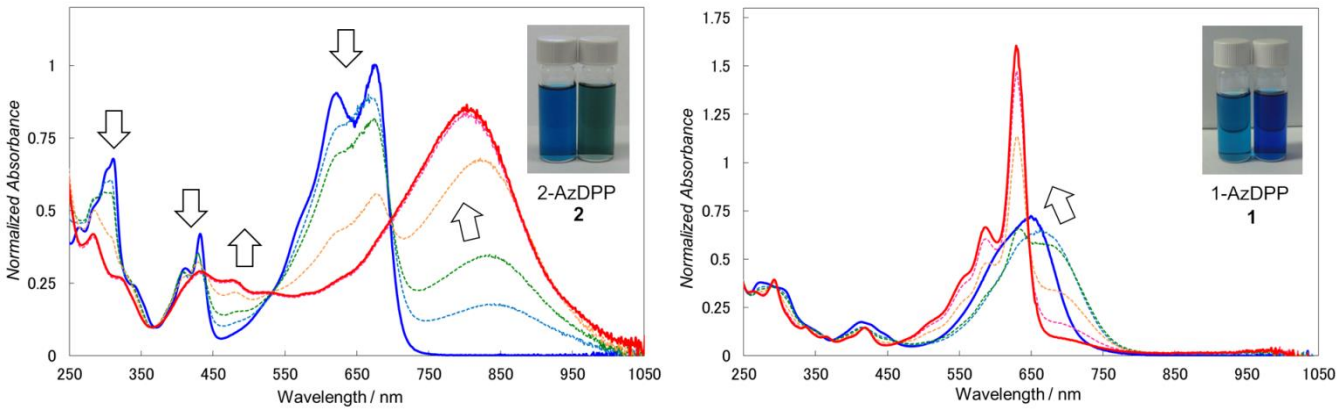

Figure 6. UV-vis spectra change in CH_2Cl_2 of 2-AzDPP **2** (left) and 1-AzDPP **1** (right) for neutral state (blue line) and after protonation by TFA (red line). Inset: photographs in the neutral state (left) and upon the addition of TFA (right).

Figure S1-S4 in ESI). As expected, the model compounds 2-AzPh, **6**, and 1-AzPh, **7**, with phenyl substituents afforded only a single protonation step even in the presence of excess TFA with the spectral changes for the isomer substituted in the 2-position, **6**, again being significantly greater than for 1-AzPh, **7** (See Figure S5 in ESI).

To gain insight into the changes in the UV-visible absorption spectra, DFT calculations on the protonated species 1-AzDPP, **1**, and 2-AzDPP, **2**, were performed. These calculations are for gas phase molecules and provide qualitative guidance of the excited state properties of these charged species. As shown in Figure 7, protonation of one azulene ring to generate the monocation $[2\text{-AzDPP}]^+$ significantly lowers both the HOMO and LUMO energy levels to -7.05 and -5.73 eV, respectively (c.f. -4.62 and -2.70 eV for the neutral 2-AzDPP). In particular, the energy level of the LUMO, which is exclusively located on DPP and the protonated azulene ring, is more strongly affected and results in a decrease in the energy gap from 1.92 eV (for 2-AzDPP (neutral)) to 1.32 eV. Interestingly, the second protonation leading to formation of the dication $[2\text{-AzDPP}]^{2+}$ affords a slight increase in the energy gap to 1.39 eV (HOMO -8.90, LUMO -7.85 eV), which is in good agreement with the UV-visible absorption change in Figure 8 and the generation of mono- and dications. The localization of frontier orbitals indicates that protonation enhances the acceptor character of the azulene units, as the LUMO is now largely located on the protonated azulene rings, while the HOMO has less contribution from this unit compared to the neutral state. Time-dependent density function theory TDDFT calculations indicate that the longest wavelength absorption bands of $[2\text{-AzDPP}]^+$ (855 nm, oscillator strength 1.42) and $[2\text{-AzDPP}]^{2+}$ (820 nm, oscillator strength 1.54) correspond to the lowest singlet-singlet excitation $S_0 \rightarrow S_1$, which consists of HOMO to LUMO transitions, respectively (Table S5-S6 in ESI). The impact of the substitution pattern is also reflected in the lowest transition energies estimated for the protonated species 1-AzDPP by TDDFT calculation: 1.80 eV (689 nm) with contributions of HOMO to LUMO+2 for the monocation

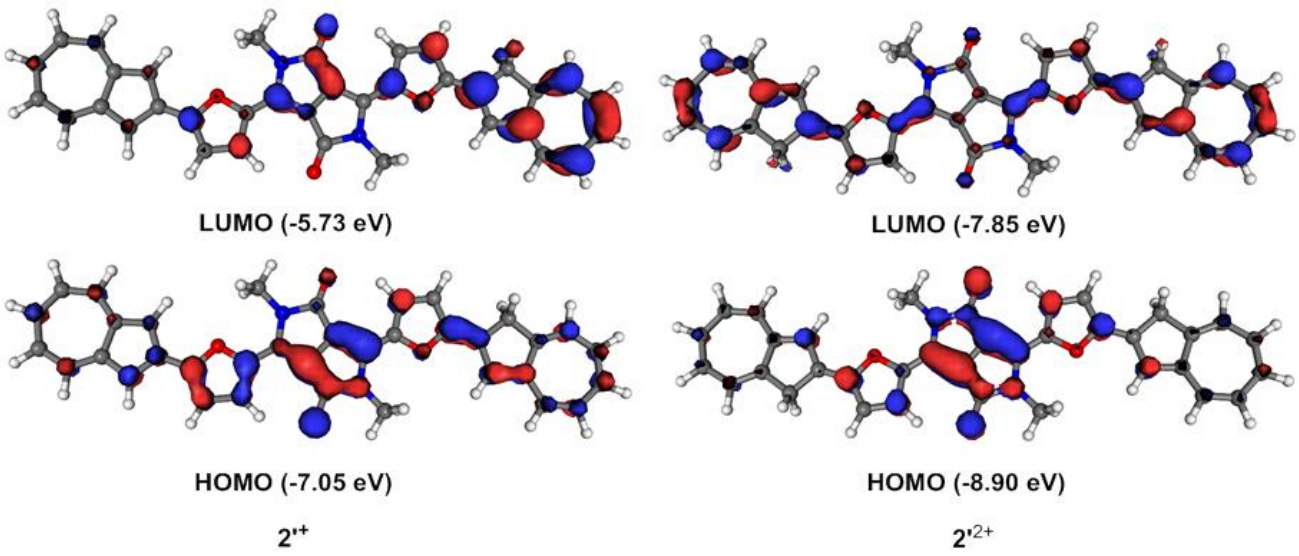

Figure 7. Optimized structure and contour plots of HOMO and LUMO of $\mathbf{2'}^+$ and $\mathbf{2'}^{2+}$.

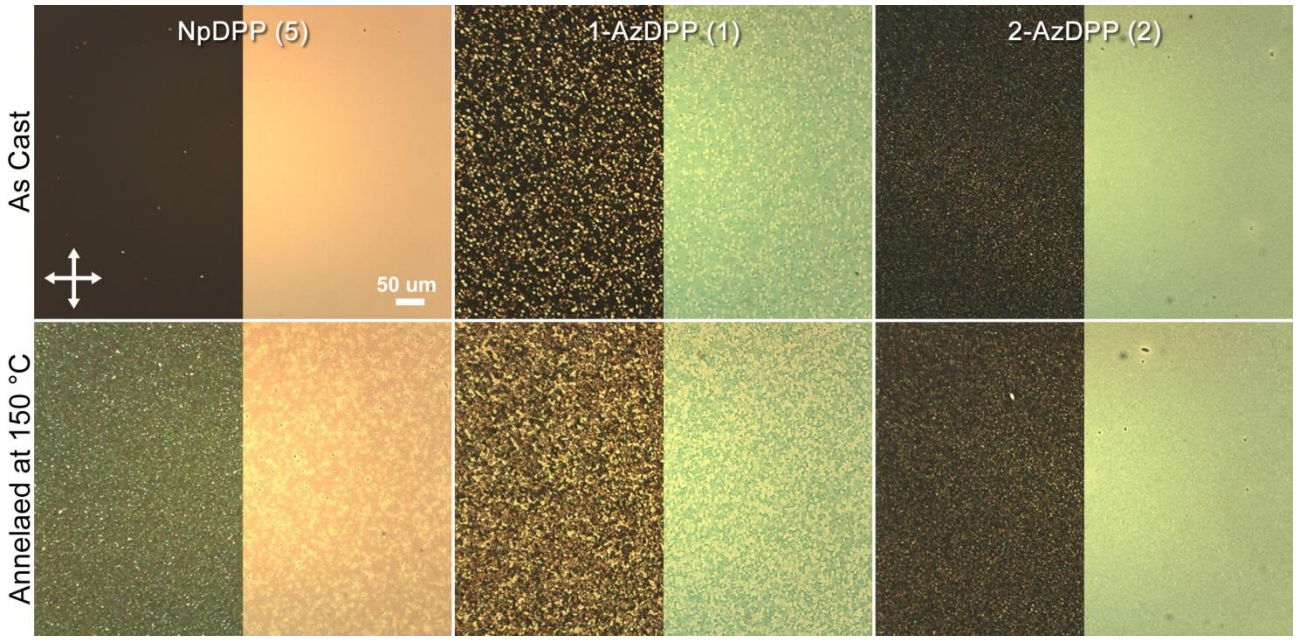

Figure 8. Transmission cross-polarized (left panel) and non-polarized (right panel) optical microscopy of thin films of NpDPP **5** (left), 1-AzDPP **1** (middle), and 2-AzDPP **2** (right) as cast (top) and annealed at 150 °C for 10 min (bottom).

$[1\text{-AzDPP}]^+$ and 2.16 eV (574 nm) with HOMO to LUMO+4 for the dication $[1\text{-AzDPP}]^{2+}$ (Table S7-S8 in ESI). It is worth mentioning that the HOMO-LUMO transition is no longer observed for either $[1\text{-AzDPP}]^+$ and $[1\text{-AzDPP}]^{2+}$, which implies that the observed lowest transition energy cannot be treated as a simple HOMO-LUMO transition in contrast to the 2-AzDPP system.

Interestingly, both azulene-DPP isomers are crystalline in solution-cast thin films which allows molecular ordering to be examined using a combination of cross-polarized and non-polarized transmission optical microscopy and high-resolution specular x-ray diffraction. For these experiments, thin films were prepared by spin coating from chlorobenzene to give continuous films (~ 100 nm in thickness). The as-cast NpDPP films had little crystalline order (indicated by the lack of birefringence in polarized optical microscopy), which improved substantially on thermal annealing (Figure 8). This interpretation is also supported by high resolution specular x-ray diffractograms that reveal two broad, out-of-plane peaks centered at 0.33 and 0.58 $Å^{-1}$ for the as-cast films and multiple strong peaks after annealing (Figure 9). Replacement of the naphthalene unit with an azulene moiety connected through the 2-position, 2-AzDPP **2**, and results in crystalline films both as-cast and after annealing. The shifts in the peak positions from

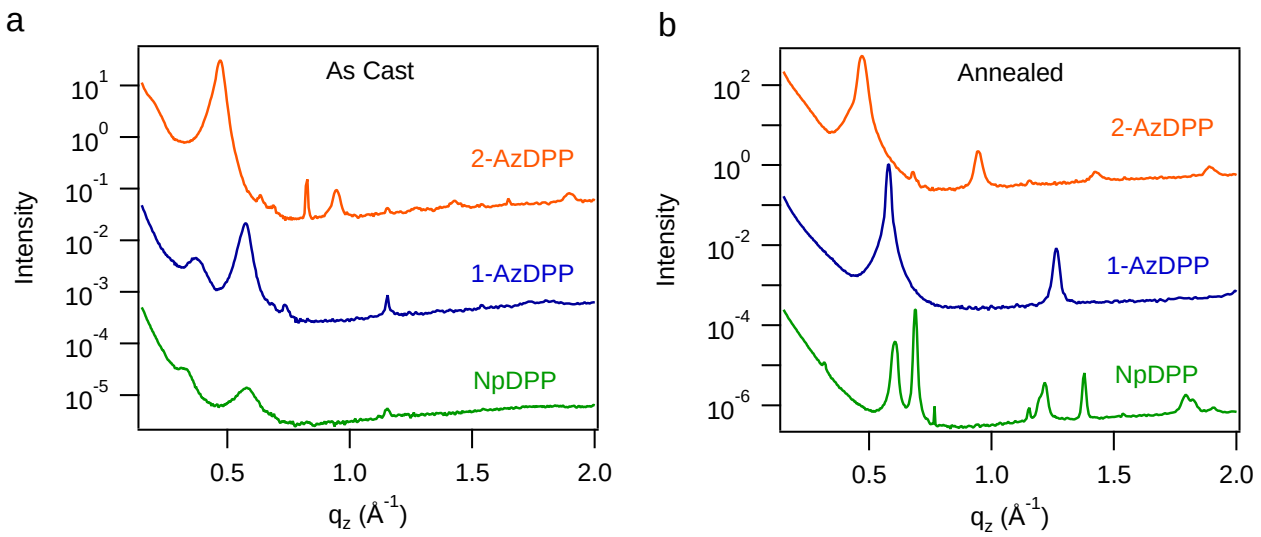

Figure 9. High-resolution specular x-ray diffraction of thin films (a) as cast and (b) after annealing at 150 °C for 10 min.

the as-cast to annealed state indicate that the as-cast and annealed films have either differing polymorphic structures or that the texture of the crystallites changes upon annealing. The isomer, 1-AzDPP **1**, was observed to have the largest birefringent domain size and the largest crystallite correlation length. Specifically, from the peak centered at 0.58 $Å^{-1}$ for 1-AzDPP **1** and 0.47 $Å^{-1}$ for 2-AzDPP **2**, we find the crystallite correlation length after annealing to be 26 nm and 9 nm, respectively. Interestingly, thin film absorption spectra also indicate increased ordering in the solid state with the lowest energy peak maxima red-shifted by 105 nm for **1** and 53 nm for **2** compared to absorption measurements in solution (Figure S6 in ESI). While the exact mechanism for this difference in molecular ordering with isomer structure is not clear at the present, it is plausible that the partial dipole moments of the azulene units may promote self-assembly and π–π stacking, improving the crystalline order of the thin films.

Conclusions

In summary, three isomeric DPP conjugates bearing azulene or naphthalene substituents have been designed and synthesized employing the direct C-H activation of azulene in concert with palladium-catalyzed Suzuki-Miyaura cross-coupling reactions. The band gap of these DPP conjugates could be tuned by the choice of azulene or naphthalene units and their substitution pattern. Theoretical calculations provided strong support for the observed structure/property relationships which showed that when the DPP unit is conjugated through the 2-position of the azulene ring, a stabilized LUMO energy level and consequently a narrower energy gap is obtained when compared with the other isomers. This is in sharp contrast to that observed for π-systems extended by annulation with traditional aromatic units where destabilization of HOMO is a major reason for decreased band-gaps. Furthermore, the introduction of the azulene units provide a partial dipole moment to the π-conjugated system, which influences planarity, molecular self-assembly and crystallization during thin-film formation. These results demonstrate the potential of azulenes substituted through the 2-position as a building block for the rational design of visible light absorbing conjugated materials with ordered morphologies and stimuli-responsiveness.

Acknowledgements

This work was partially supported by DOE Basic Energy Science under award DE-SC0005414 (M.M., M.L.C., M.J.R. and C.J.H.), the NSF PREM program between UCSB and UTEP (DMR-1205302) (N.D.T., M.L.C., and C.J.H.) and the MRSEC Program of the NSF under award no. DMR-1121053 (M.M., S.K., M.J.R., and C.J.H.). M.M. thanks the JSPS Research Fellowships for Young Scientists and also thanks Dr. Kei Murata (Tokyo Institute of Technology) and Dr. Akiko Inagaki (Tokyo Metropolitan University) for the helpful discussions on DFT calculation.

Notes and references

[a]Materials Research Laboratory, [b]Materials Department, and [c]Department of Chemistry and Biochemistry, University of California, Santa Barbara, Santa Barbara, California 93106, United States. [d]Division of Chemistry and Biotechnology, Graduate School of Natural Science and Technology, Okayama University, 3-1-1 Tsushimanaka, Kita-ku, Okayama 700-8530, Japan.

Electronic Supplementary Information (ESI) available: [details]. See DOI: 10.1039/b000000x/

1. a) P. Bäuerle, In *Electronic Materials: The Oligomer Approach*; Müllen, K.; Wegner, G., Eds.; Wiley-VCH: Weinheim, Germany, 1998; Chapter 2; b) T. A. Skotheim, J. R. Reynolds, *Handbook of Conducting Polymers*, 3rd ed.; CRC Press: Boca Raton, FL, 2007; c) Y. Shirota, H. Kageyama, *Chem. Rev.* **2007**, *107*, 953-1010; d) A. R. Murphy, J. M. J. Fréchet, *Chem. Rev.* **2007**, *107*, 1066-1096; e) J. Zaumseil, H. Sirringhaus, *Chem. Rev.* **2007**, *107*, 1296-1323; (e) C. Duan, F. Huang; Y. Cao *J. Mater. Chem.* **2012**, *22*, 10416-10434.
2. a) J. Fabian, H. Nakazumi, M. Matsuoka, *Chem. Rev.* **1992**, *92*, 1197-1226; b) G. Qian, Z. Y. Wang, *Chem. Asian J.* **2010**, *5*, 1006-1029; c) T. Weil, T. Vosch, J. Hofkens, K. Peneva, K. Müllen, *Angew. Chem. Int. Ed.* **2010**, *49*, 9068-9093.
3. J. Liu, B. Walker, A. Tamayo, Y. Zhang, T.-Q. Nguyen, *Adv. Funct. Mater.* **2013**, *23*, 47–56.
4. a) K.-P. Zeller, *Azulene*. In *Houben-Weyl: Methoden der Organischen Chemie*, 4th ed.; Georg Thieme: Stuttgart, Germany, 1985; Vol. V, Part 2C, pp 127; b) J. Michl, E.W. Thulstrup, *Tetrahedron* **1976**, *32*, 205-209; c) P. Foggi, F. V. R. Neuwahl, L. Moroni, P. R. Salvi, *J. Phys. Chem. A* **2003**, *107*, 1689-1696; d) S. V. Shevyakov, H. Li, R. Muthyala, A. E. Asato, J. C. Croney, D. M. Jameson, R. S. H. Liu, *J. Phys. Chem. A* **2003**, *107*, 3295-3299.
5. a) J. E. Frey, A. M. Andrews, S . D. Combs, S . P. Edens, J. J. Puckett, R. E. Seagle, L. A. Torreano, *J. Org. Chem.* **1992**, *57*, 6460-6466; b) S. E. Estdale, R. Brettle, D. A. Dummur, C. M. Marson, *J. Mater. Chem.* **1997**, *7*, 391-401; c) M. Porsch, G . Sigl-Seifert, J. Daub, *Adv. Mater.* **1997**, 9, 635-639; d) S. Schmitt, M. Baumgarten, J. Simon, K. Hafner, *Angew. Chem. Int. Ed.* **1998**, *37*, 1077-1081; e) T. Mrozek, H. Gorner, J. Daub, *Chem. Eur. J.* **2001**, *7*, 1028-1040; f) S. Ito, H. Inabe, N . Morita, K. Ohta, T . Kitamura, K. Imafuku, *J. Am. Chem. Soc.* **2003**, 125, 1669-1680; g) F. Wang, Y.-H. Lai, M.-Y. Han, *Macromolecules* **2004**, *37*, 3222-3230; h) T. Zielinski, M. Kedziorek, J. Jurczak, *Tetrahedron Lett.* **2005**, *46*, 6231-6234; i) H. Salman, Y. Abraham, S. Tal, S. Meltzman, M. Kapon, N. Tessler, S. Speiser, Y. Eichen, *Eur. J. Org. Chem.* **2005**, 2207-2212; j) C.Y. Chiu, H.B. Wang, F.G. Brunetti, F. Wudl, C.J. Hawker, *Angew. Chem. Int. Ed.* **2014**, *53*, 3996-4000; k) J. Xia, B. Capozzi, S. Wei, M. Strange, A. Batra, J. R. Moreno, R. J. Amir, E. Amir, G. C. Solomon, L. Venkataraman, L. M. Campos, *Nano Lett.* **2014**, *14*, 2941-2945.
6. a) K. Kurotobi, K. S. Kim, S. B. Noh, D. Kim, A. Osuka, *Angew. Chem. Int. Ed.* **2006**, *45*, 3944-3947; b) A. Muranaka, M. Yonehara, M. Uchiyama, *J. Am. Chem. Soc.* **2010**, *132*, 7844-7845; c) M. Ince, J. Bartelmess, D. Kiessling, K. Dirian, M. V. Martínez-Díaz, T. Torres, D. M. Guldi, *Chem. Sci.* **2012**, *3*, 1472-1480.
7. Azulene derivatives having push-pull substituents have been utilized as nonlinear optical (NLO) materials. See; a) P. G. Lacroix, I. Malfant,G. Iftime, A. C. Razus, K. Nakatani, J. A. Delaire, *Chem. Eur. J.* **2000**, *6*, 2599-2608; b) C. Lambert, G. Noell, M. Zabel, F.

Hampel, E. Schmaelzlin, C. Braeuchle, K. Meerholz, *Chem. Eur. J.* **2003**, *9*, 4232-4239; c) L. Cristian, I. Sasaki, P. G. Lacroix, B. Donnadieu, I. Asselberghs, K. Clays, A. C. Razus, *Chem. Mater.* **2004**, *16*, 3543-3551; d) Y. Yamaguchi, K. Ogawa, K.-i. Nakayama, Y. Ohba, H. Katagiri, *J. Am. Chem. Soc.* **2013**, *135*, 19095-19098.

8. a) E. Amir, R. J. Amir, L. M. Campos, C. J. Hawker, *J. Am. Chem. Soc.* **2011**, *133*, 10046-10049; b) M. Murai, E. Amir, R. Amir, C. J. Hawker, *Chem. Sci.* **2012**, *3*, 2721-2725.
9. For recent examples, see: a) G. C. Welch, R. Coffin, J. Peet, G. C. Bazan, *J. Am. Chem. Soc.* **2009**, *131*, 10802-10803; b) A. Job, A. Wakamiya, G. Kehr, G. Erker, S. Yamaguchi, *Org. Lett.* **2010**, *12*, 5470-5473; c) G. C. Welch, G. C. Bazan, *J. Am. Chem. Soc*. **2011**, *133*, 4632-4644; d) P. Zalar, Z. B. Henson, G. C. Welch, G. C. Bazan, T.-Q. Nguyen, *Angew. Chem. Int. Ed.* **2012**, *51*, 7495-7498; e) T. M. McCormick, A. A. Jahnke, A. J. Lough, D. S. Seferos, *J. Am. Chem. Soc.* **2012**, *134*, 3542-3548; f) M.A. Naik, S. Patil. *J. Polym. Sci. Part A; Polym. Chem*. **2013**, *51*, 4241–4260.
10. For reviews on diketopyrrolopyrroles (DPPs), see: a) Z. Hao, A. Iqbal, *Chem. Soc. Rev.* **1997**, *26*, 203-213; b) O. Wallquist, R. Lenz, *Macromol. Symp.* **2002**, *187*, 617-629; c) O. Wallquist, In *High-Performance Pigments*; Smith, H. M., Ed.; Wiley-VCH: Weinheim, 2002, 159-184; d) B. Walker, C. Kim, T.-Q. Nguyen, *Chem. Mater.* **2011**, *23*, 470-482; e) M. J. Robb, S.-Y. Ku, F. G. Brunetti, C. J. Hawker, *J. Polym. Sci. Part A; Polym. Chem*. **2013**, *51*, 1263-1271; f) J.W. Rumer, S.-Y. Dai, M. Levick, L. Biniek, D.J. Procter, I. McCulloch, *J. Polym. Sci. Part A; Polym. Chem.* **2013**, *51*, 1285–1291; g) Y. Han, L. Chen, Y. Chen, *J. Polym. Sci. Part A; Polym. Chem.* **2013**, *51*, 258–266.
11. For selected examples, see: a) T. Umeyama, T. Takamatsu, N. Tezuka, Y. Matano, Y. Araki, T. Wada, O. Yoshikawa, T. Sagawa, S. Yoshikawa, H. Imahori, *J. Phys. Chem. C* **2009**, *113*, 10798-10806; b) C. H. Woo, P. M. Beaujuge, T. W. Holcombe, O. P. Lee, J. M. J. Fréchet, *J. Am. Chem. Soc.* **2010**, *132*, 15547-15549; c) U. H. F. Bunz, *Angew. Chem. Int. Ed.* **2010**, *49*, 5037-5040; d) A. T. Yiu, P. M. Beaujuge, O. P. Lee, C. H. Woo, M. F. Toney, J. M. J. Fréchet, *J. Am. Chem. Soc.* **2012**, *134*, 2180-2185.
12. Introduction of electron-donating substituents on the 2-position of azulene rings have been reported. See: a) G. Nöll, J. Daub, M. Lutz, K. Rurack, *J. Org. Chem.* **2011**, *76*, 4859-4873; b) Y. Yamaguchi, Y. Maruya, H. Katagiri, K. Nakayama, Y. Ohba, *Org. Lett.* **2012**, *14*, 2316-2319.
13. a) R. Yokoyama, S. Ito, M. Watanabe, N. Harada, C. Kabuto, N. Morita, *J. Chem. Soc*., *Perkin Trans. 1*, **2001**, 2257-2261; b) S, Ito, A. Nomura, N. Morita, C. Kabuto, H. Kobayashi, S Maejima, K. Fujimori, M. Yasunami, *J. Org. Chem.* **2002**, *67*, 7295-7302**;** c) J. Zhang, S. Petoud, *Chem. Eur. J.* **2008**, *14*, 1264-1272.
14. a) T. Nozoe, S. Seto, S. Matsumura, Y. Murase, *Bull. Chem. Soc. Jpn.* **1962**, *35*, 1179; b) R. N. McDonald, J. M. Richmond, J. R. Curtis, H. E. Petty, T. L. Hoskins, *J. Org. Chem.* **1976**, *41*, 1811.
15. A. G. Anderson Jr., J. A. Nelson, J. J. Tazuma, *J. Am. Chem. Soc.* **1953**, *75*, 4980.
16. a) K. Kurotobi, M. Miyauchi, K. Takakura, T. Murafuji, Y. Sugihara, *Eur. J. Org. Chem.* **2003**, 3663-3665. b) M. Fujinaga, T. Murafuji, K. Kurotobi, Y. Sugihara, *Tetrahedron* **2009**, *65*, 7115-7121.
17. For reviews on direct borylation of aromatic C-H bonds, see: a) N. Miyaura, *Bull. Chem. Soc. Japan*. **2008**, *81*, 1535-1553. b) I. A. I. Mkhalid, J. H. Barnard, T. B. Marder, J. M. Murphy, J. F. Hartwig, *Chem. Rev*. **2010,** *110*, 890-931.
18. Vibronic structures of UV-visible absorption were not observed (or poorly resolved) for compounds **1** and **7** due in part to their low symmetry compared with **2**, **4**, and **6**. UV-visible absorption spectra of **1**, **2**, **4**, and **5** in solution-cast thin films are shown in Figure S6 in the ESI.
19. The absolute quantum yield of **5** determined by using a calibrated integrating sphere system was 17%.
20. Fluorescence of DPP-azulene conjugates **1** and **2** was not observed even in solution-cast thin films.
21. Z. R. Grabowski, K. Rotkiewicz, W. Rettig, *Chem. Rev.* **2003**, *103*, 3899-4032.
22. The emission of azulene can be observed with very low quantum efficiency and very short lifetime. See, for example: a) M. J. Bearpark , F. Bernardi, S. Clifford, M. Olivucci, M. A. Robb, B. R. Smith, T. Vreven, *J. Am. Chem. Soc.* **1996**, *118*, 169-175; b) S. Y. Kim, G. Y. Lee, S. Y. Han, M. Lee, *Chem. Phys. Lett.* **2000**, *318*, 63-68.
23. The emission quantum yield of azulene is known to be very low due to dominant transition from the excited S_2 state to the S_0 state (*i.e.* violation of Kasha's rule). For Kasha's rule, see: Kasha, M. *Discuss. Faraday Soc.* **1950**, *9*, 14.
24. a) J. Michl, E. W. Thulstrup, *Tetrahedron* **1976**, *32*, 205-209; b) D. M. Lemal, G. D. J. Goldman, *J. Chem. Educ.* **1988**, *65*, 923-925.
25. Spectral and color changes upon the addition of TFA similar to those in CH_2Cl_2 are also observed in toluene, whereas no change was observed in other solvents such as THF and DMF.
26. a) M. Porsch, G. Sigl-Seifert, J. Daub, *Adv. Mater.* **1997**, *9*, 635-639; b) F. Wang, Y.-H. Lai, N. M. Kocherginsky, Y. Y. Koteski, *Org. Lett.* **2003**, *5*, 995-998; c) F. Wang, Y.-H. Lai, *Macromolecules* **2003**, *36*, 536-538; d) X. Wang, J.-K. Ng, P. Jia, T. Lin, C. M. Cho, J. Xu, X. Lu, C. He, *Macromolecules* **2009**, *42*, 5534-5544.
27. Radicals in the azulenium radical cation states are known to localize on the five-membered rings. See: a) K. Tanaka, M. Toriumi, S. Wang, T. Yamabe, *Polymer J.* **1990**, 22, 1001-1006; b) G. Nöll, C. Lambert, M. Lynch, M. Porsch, J. Daub, *J. Phys. Chem. C* **2008**, *112*, 2156-2164.

Graphical Abstract